Influence of Metal Nanoparticles on the Structural and Optical Properties of the MnO_2 Thin Film

Stacy A Lynrah
Electronics and Communication Engineering Department
National Institute of Technology, Nagaland
Dimapur, Nagaland
stacy038@gmail.com

L. Vigneash
Electronics and Communication Engineering Department
Arjun College of Technology, Coimbatore, Tamil Nadu
lvigneash2504@gmail.com

P. Chinnamuthu
Electronics and Communication Engineering Department
National Institute of Technology, Nagaland
Dimapur, Nagaland
chinnamuthu@nitnagaland.ac.in

Ying Ying Lim
Electrical, electronics and communication engineering Department
Tokyo City University
Tokyo, Japan
ying@tcu.ac.jp

***Abstract*— This work aims to concisely overview the relationship between metal nanoparticles and MnO_2 thin films. The electron beam evaporation technique deposited MnO_2 Thin Film (TF) decorated with titanium (Ti), Gold (Au), and silver (Ag) nanoparticles (NP). The study involved the analysis of the structural and optical properties of a MnO_2 thin film decorated with nanoparticles (Au, Ag, Ti). XRD reveals that the MnO_2 TF and the metal nanoparticles are crystalline. The AFM analysis of Ti NP/MnO_2 TF, Ag NP/MnO_2 TF, and Au NP/MnO_2 TF with a value of 0.19 nm, 0.18 nm, and 0.17 nm, respectively Reflectance measurement unveils the Au NP/MnO_2 TF, Ag NP/MnO_2 TF, and Ti NP/MnO_2 TF bandgap, which are 3.64 eV, 3.37 eV, and 3.12 eV at 340 nm, 367 nm, and 397 nm. PL emission shows that Au NP/MnO_2 TF has more emission than Ag NP/MnO_2 TF and Ti NP/MnO_2 TF.**

Keywords*— Silver, Gold, Titanium, MnO_2, Thin Film, structural, optical properties.

I. Introduction

The advent of nanotechnology has sparked a transformative revolution across multiple scientific and technological domains, offering distinctive properties and functionalities at the nanoscale. Noble metal nanoparticles, including Gold (Au), Silver (Ag), Platinum (Pt) nanoparticles, and many others, have indeed garnered significant research interest worldwide. Metal nanoparticles exhibit plasmonic effects, such as localized surface plasmon resonance (LSPR), which can manipulate and enhance light absorption and scattering, as shown in Fig.1. The electron cloud surrounding the nanoparticles plays a crucial role in this phenomenon. The interaction between the incident electromagnetic field and the electrons in the metal nanoparticles results in the excitation of surface plasmons (collective vibrations of the conduction electrons) [1]. Metals are favored for plasmonic because they exhibit a strong interaction between light and electrons, allowing for efficient coupling of light energy to surface plasmons. They have a wide range of optical responses across the electromagnetic spectrum, ranging from ultraviolet to infrared [2]. In addition, they have high electrical conductivity, and depending on the specific application, different metals can be used for tailoring plasmonic properties. On the other hand, the versatility and broad range of properties exhibited by metal oxide thin films have sparked considerable interest, positioning them as promising materials with extensive applications across diverse fields.

Incorporating metal nanoparticles (NPs) into semiconductors or oxide materials produces a synergetic effect. They can significantly change the optical properties of both the nanoparticles and the host materials. By combining these two types of nanoparticles, the optical properties can be tailored, resulting in synergistic effects that enable advanced applications in sensing, imaging, and photovoltaics [3]. These nanoparticles can be engineered to manipulate and control the behavior of the surface plasmons. The interaction of incident light with the metal nanoparticles increases light absorption, optical path length, and spectral tunability by controlling their size, shape, and material composition [4]. The LSPR spectrum of a metallic nanoparticle includes both scattering and absorption components, which are strongly dependent on particle morphology, size, and composition. The high electromagnetic field intensity around the nanoparticles enhances the interaction between light and the thin film, resulting in a higher probability of light absorption. As each metal nanoparticle exhibits its characteristic resonance wavelength, the combined effect enhances light absorption across a broad range of wavelengths [5]. Moreover, the LSPR effect can lead to a shift in the reflectance minimum of material. This shift occurs when the incident light matches the resonance condition of the LSPR, resulting in a decrease in reflectance at specific wavelengths.

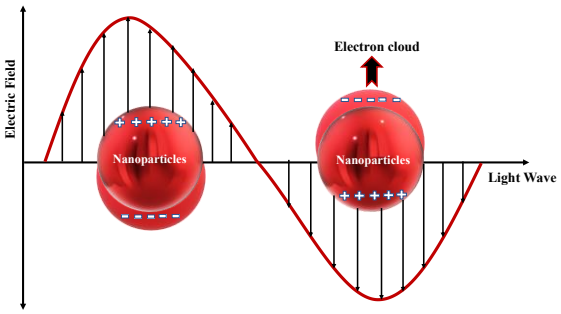

Fig. 1: LSPR effect of metal nanoparticles.

The combination of metal NP with metal oxide TF can modify its bandgap. Different metal nanoparticles have

The work is sponsored by the SERB, DST, Government of India (EEQ/2021/000507).

distinct optical properties. By selecting specific metal nanoparticle materials, it is possible to tailor the absorption properties of the metal oxide thin film to match desired requirements [6].

In this study, we aim to investigate the influence of metal nanoparticles (Gold, Silver, Titanium) on the structural and optical characteristics of MnO_2 thin films. The MnO_2 TF decorated with metal NP was grown by a non-catalytic method, i.e., electron beam evaporation technique, as shown in Fig. 2. Here, precise control for the growth of MnO_2 TF incorporated with metal NP can be done using this method. The work focus has been done on the structural and optical studies of different metals decorated with TF. The findings of this study will yield valuable insights into the design and optimization of metal-MnO_2 TF for diverse applications such as sensor and optoelectronics applications.

II. Experimental Details

Silicon substrates cut into 1× 1 cm was taken. They were cleaned by a non-destructive process, i.e., ultrasonically in acetone, methanol, and DI water. The ultrasonic cleaner and the solvent's cleaning action enhance the cleaning efficiency. They are kept in a substrate holder and transferred to the electron beam chamber for deposition. MnO_2 granules of 99.99% purity (Ultrananotech Private Limited) was used for depositing the thin film. The Metal NP (Au, Ag, and Ti NP) are subsequently deposited on the MnO_2 TF, as shown in Fig. 2. Both the TF and NP were deposited at a rate of 1.0 Å/s in the chamber with the base pressure of 5×10^{-5} mbar. Each deposition was done approximately for 10 mins, with a thickness of ~50 nm. This process is continued until a thickness of 500 nm is obtained. For the NP, deposition of 8 nm was done for all the Ag, Au, and Ti NP. A quartz crystal monitor can measure the deposition rate by monitoring the change in frequency of a quartz crystal sensor placed near the substrate.

The XRD characterization was done on a Rigaku Smart Lab guidance using CuKα radiation (λ = 0.154). Hitachi, F-7000, performed the reflectance measurement. The photoluminescence (PL) Analysis was done at an excitation wavelength of 250 nm using an F-7000 fluorescence spectrophotometer. Surface analysis was performed using AFM analysis (Hitachi High-Tech (former SII Nano Technology)) was done for surface analysis.

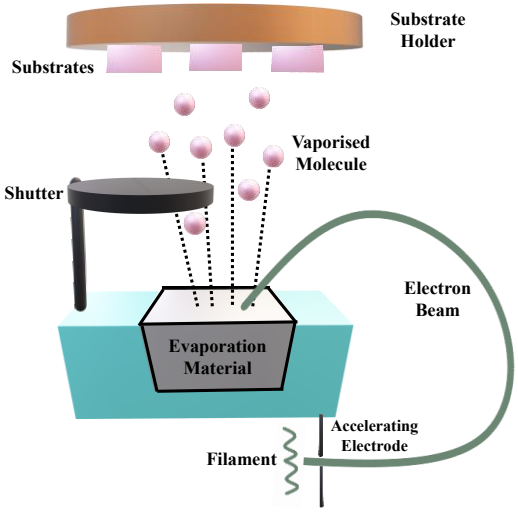

Fig.2: Schematic diagram of the e-beam evaporator.

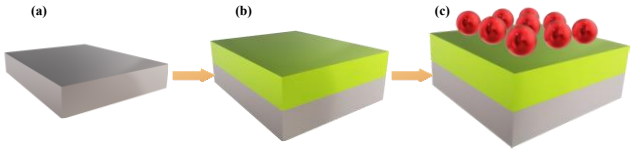

Fig. 3: Schematic diagram of an (a)Substrate, (b) MnO_2 Thin film deposited on a substrate, and (c) Metal nanoparticles (Au/Ag/Ti) deposited on thin film.

III. Results and Discussions

XRD characterization determines the crystalline properties of the Au NP/MnO_2 TF, Ag NP/ MnO_2 TF, and Ti NP/MnO_2 TF. Both the metal nanoparticles and the MnO_2 TF are crystalline. The diffracted peak of the metal NP and the MnO_2 TF are assigned with different symbols, as shown in Fig.4 [7, 8, 9].

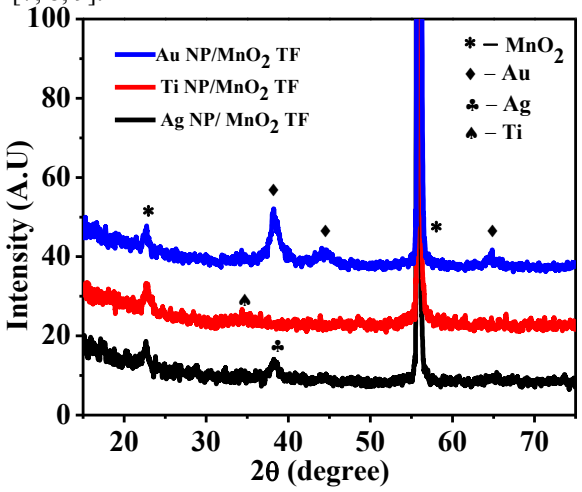

Fig. 4 XRD of Au NP/MnO_2 TF, Ag NP/ MnO_2 TF, and Ti NP/MnO_2 TF.

An AFM analysis of a thin film decorated with nanoparticles typically provides a high-resolution topographic image of the sample's surface, as shown in Fig. The images reveal the surface roughness and morphology of Ti NP/MnO_2 TF, Ag NP/MnO_2 TF, and Au NP/MnO_2 TF with a value of 0.19 nm, 0.18 nm, and 0.17 nm, respectively. The higher surface roughness observed in Ti nanoparticles, as compared to Ag and Au nanoparticles, may be attributed to Ti's lower electronegativity than Ag and Au.[10]. Metals with lower electronegativity values are more reactive and prone to oxidation. This increased reactivity can result in the formation of rougher surface oxides.

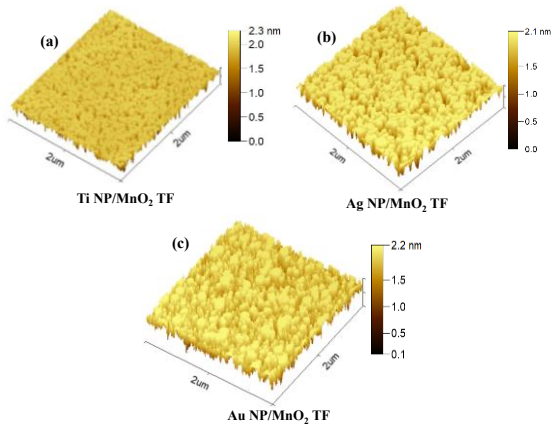

Fig. 5: AFM analysis of Ti NP/MnO_2 TF, Ag NP/MnO_2 TF, and Au NP/MnO_2 TF

The energy bandgap can be found out from the reflectance spectra shown in Fig. 6. The reflectance spectra show several fringes in all three MnO_2 TF decorated with metal NP.

Usually, when incident light interacts with the metal oxide thin film and the nanoparticles, it undergoes multiple reflections between these interfaces. This results in forming interference patterns, represented by the Fabry-Perot interference fringes. Ag, Au, or Ti nanoparticles on the metal oxide thin film introduce additional reflective surfaces, leading to more opportunities for light interference [11].

The nanoparticle size, spacing, and distribution are crucial in determining the interference pattern. Furthermore, the interference fringes gradually disappear in the proximity of the wavelength corresponding to the optical absorption edge. The interference fringes provide valuable information for studying these composite materials' optical behavior and performance in various applications, including optoelectronics, plasmonic, and sensing [12]. The observed figure demonstrates that the interference fringes become indiscernible at 340 nm, 367 nm, and 397 nm for Au NP/MnO_2 TF, Ag NP/ MnO_2 TF, and Ti NP/MnO_2 TF, respectively. So, the calculated bandgap energy for the obtained wavelength is 3.64 eV, 3.37 eV, and 3.12 eV, which is 340 nm, 367 nm, and 397 nm for Au NP/MnO_2 TF, Ag NP/ MnO_2 TF and Ti NP/MnO_2 TF. Compared to the bandgap of bare MnO_2, which is 2.7 eV, as reported by Pinaud [13], adding metal NP increases the bandgap overall. The enhancement/ widening of the bandgap could be due to the Moss-Burstein effect arising from Pauli's exclusion principle. This indicates that decorating the MnO_2 TF with nanoparticles can modify the bandgap of the MnO_2 TF. Due to this effect, there is an increase in the Fermi level in the conduction band since the conduction band got filled up due to the donors [14, 15]. This is another approach for tailoring the MnO_2 TF electronic and optical properties, commonly called plasmonic modification or enhancement.

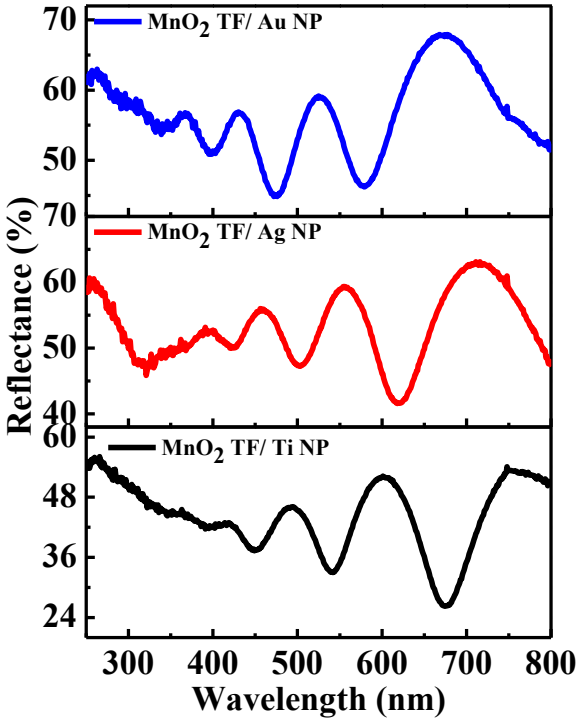

Fig. 6: Reflectance measurement of Au NP/MnO_2 TF, Ag NP/ MnO_2 TF, and Ti NP/MnO_2 TF.

Metal nanoparticles can alter the local electromagnetic field distribution near the metal oxide thin film surface. This enhanced local field can influence the radiative recombination processes, enhancing plasmon emission. Here the metal nanoparticles exhibit LSPR (Localized Surface Plasmons Resonance), which can couple with the excited states of the MnO_2 TF. The PL emission is done at an excitation wavelength of 250 nm. The PL emission is more pronounced in the Au NP/MnO_2 TF compared to Ag NP/MnO_2 TF and Ti NP/MnO_2 TF, as depicted in Fig. 7.

The transport probability of electrons to the localized surface plasmon level or the Fermi level of the metal can enhance or reduce luminescence intensity [16]. If the transported probability is high, the excited electrons can efficiently couple with the LSPs, enhancing luminescence intensity. The LSPs can enhance the local electromagnetic field, enhancing the excited state's emission rate and radiative decay. Both Au and Ag are known to exhibit good electron transport behavior. However, in this case, Au NP/MnO_2 TF has more PL emission as compared to Ag NP/ MnO_2 TF and Ti NP/ MnO_2 TF, which could be due to more transport probability of Au as compared to Ag and also due to the radiative recombination [17].

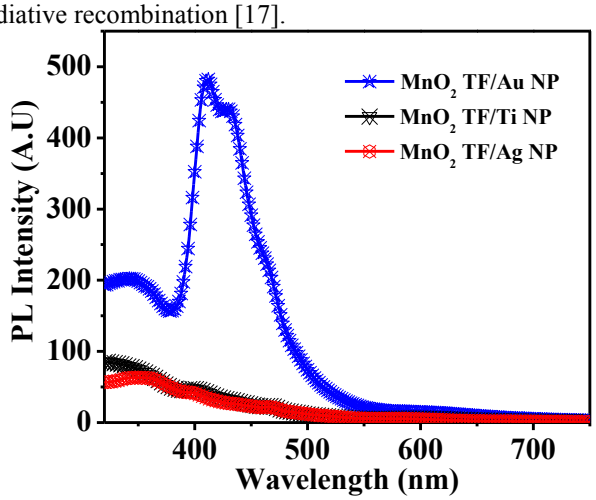

Fig. 7: PL emission of Au NP/MnO_2 TF, Ag NP/ MnO_2 TF and Ti NP/MnO_2 TF.

IV. CONCLUSION

In conclusion, adding NP to the MnO_2 TF can modify their structural and optical properties. The metal NP and the MnO_2 TF are crystalline. The AFM analysis reveals that Ti Np's surface roughness is higher than that of Au and Ag NP, which could be due to the less electronegativity of Ti. The bandgap got modified after the addition of the metal NP. The bandgap obtained is 3.64 eV, 3.37eV, and 3.12 eV at 340 nm, 367 nm, and 397 nm for Au NP/MnO_2 TF, Ag NP/ MnO_2 TF, and Ti NP/MnO_2 TF, respectively. The PL emission intensity of Au NP/MnO_2 TF is higher than the Ag NP/MnO_2 TF and Ti NP/MnO_2 TF. The unique properties of Au NP, such as their LSPR and good stability, can contribute to enhanced optical properties and better performance in specific optoelectronic or sensing applications.

ACKNOWLEDGMENT

The authors are grateful to the Physics Department, NIT Nagaland, for XRD measurement, the NIT Manipur for PL Measurement, and NIT Nagaland for providing the facilities.

REFERENCES

[1] S. Kumar, R.Singh, Q. Yang, S. Cheng, B. Zhang, and B. Kumar Kaushik. "Highly sensitive, selective and portable sensor probe using

germanium-doped photosensitive optical fiber for ascorbic acid detection." *IEEE Sensors Journal,* vol. 21, no. 1, pp. 62-70, 2020.

[2] Q. Li, J. Meng, J. Huang, and Z. Li. "Plasmon-induced pyro-phototronic effect enhancement in self-powered UV–vis detection with a ZnO/CuO p–n junction device." *Advanced Functional Materials,* vol. 32, no. 7, pp. 2108903, 2022.

[3] N. Kumar, H. B. Lee, S. Hwang, T.-W. Kim, and J.-W. Kang. "Fabrication of plasmonic gold-nanoparticle-transition metal oxides thin films for optoelectronic applications." *Journal of Alloys and Compounds,* vol. 775, pp. 39-50, 2019).

[4] H. A. Atwater, and A. Polman. "Plasmonics for improved photovoltaic devices." *Nature Materials,* vol. 9, no. 3, pp. 205-213, 2010.

[5] S. H. Raad, Zahra Atlasbaf, and Carlos J. Zapata-Rodríguez. "Broadband absorption using all-graphene grating-coupled nanoparticles on a reflector." *Scientific Reports,* vol.10, no. 1, pp. 19060 (1-15), 2020.

[6] J. Su, D. Liu, L. Sun, G. Chen, C. Ma, Q. Zhang, and X. Li. "Plasmonic Nanostructures for Broadband Solar Absorption Based on Synergistic Effect of Multiple Absorption Mechanisms." *Nanomaterials,* vol. 12, no. 24, pp. 4456, 2022.

[7] S.A. Lynrah, P. Pheiroijam and P. Chinnamuthu, Scrutinizing and Collating the Broadband Photo-Detection Properties of Isotype n-MnO_2/TiO_2 Nanostructure. IEEE Sensors Journal, vol. 2, no. 2, pp.1485-1492, 2020.

[8] S. S. Godipurge, S. Yallappa, N. J. Biradar, J. S. Biradar, B. L. Dhananjaya, G. Hegde, K. Jagadish, and G. Hegde. "A facile and green strategy for the synthesis of Au, Ag and Au–Ag alloy nanoparticles using aerial parts of R. hypocrateriformis extract and their biological evaluation." *Enzyme and microbial technology,* vol. 95 pp. 174-184, 2016.

[9] V. Y. Zadorozhnyy, X. Shi, M. V. Gorshenkov, D. S. Kozak, T. Wada, D. V. Louzguine-Luzgin, A. Inoue, and H. Kato. "Ti–Ag–Pd alloy with good mechanical properties and high potential for biological applications." *Scientific reports,* vol. 6, no. 1, pp.1-9, 2016.

[10] A. Jog, E. Milosevic, P. Zheng, and D. Gall. "Effect of electronegativity on electron surface scattering in thin metal layers." *Applied Physics Letters,* vol. 120, no. 4, 2022.

[11] Afzal, Naveed, and Mutharasu Devarajan. "Fabrication and characterization of $In_{0.83}$ $Al_{0.17}$ N based MSM visible photodiode." *The European Physical Journal Applied Physics,* vol. 76, no. 1, pp. 10101 (1-8), 2016.

[12] A. A. Ahmed, N. Afzal, M. Devarajan, and S. Subramani. "Structural, morphological, optical and electrical properties of NiO films prepared on Si (100) and glass substrates at different thicknesses." *Materials Research Express,* vol. 3, no. 11, pp. 116405, 2016.

[13] B. A. Pinaud, Z. Chen, D. N. Abram, and T. F. Jaramillo. "Thin films of sodium birnessite-type MnO_2: optical properties, electronic band structure, and solar photoelectrochemistry." *The Journal of Physical Chemistry C,* vol. 115, no. 23, pp. 11830-11838, 2011.

[14] K. G. Saw,, N. M. Aznan, F. K. Yam, S. S. Ng, and S. Y. Pung. "New insights on the Burstein-moss shift and band gap narrowing in indium-doped zinc oxide thin films." *PloS one,* vol. 10, no. 10, pp. e0141180 (1-17), 2015.

[15] H. W. Lee, S. P. Lau, Y. G. Wang, K. Y. Tse, H. H. Hng, and B. K. Tay. "Structural, electrical and optical properties of Al-doped ZnO thin films prepared by filtered cathodic vacuum arc technique." *Journal of Crystal Growth,* vol. 268, no. 3-4, pp. 596-601, 2004.

[16] C. Huo, H. Jiang, Y. Lu, S. Han, F. Jia, Y. Zeng, P. Cao, W. Liu, X., Liu, X. Wangying, and Zhu, D., Tunable photoluminescence effect from ZnO films of Ag-decorated localized surface plasmon resonance by varying positions of Ag nanoparticles, *Materials Research Bulletin*, vol. *111*, pp.17-23, 2019.

[17] Cheng, C. W., E. J. Sie, B. Liu, C. H. A. Huan, T. C. Sum, H. D. Sun, and H. J. Fan. "Surface plasmon enhanced band edge luminescence of ZnO nanorods by capping Au nanoparticles." *Applied Physics Letters,* vol. 96, no. 7, pp. 071107 (1-3), 2010.